ORIGINAL ARTICLE

Acute stress modulates noradrenergic signaling in the ventral tegmental area-amygdalar circuit

Michal Kielbinski[1] | Joanna Bernacka[1,2] | Katarzyna Zajda[1] | Agnieszka Wawrzczak-Bargieła[2] | Marzena Maćkowiak[2] | Ryszard Przewlocki[3] | Wojciech Solecki[1]

[1]Department of Neurobiology and Neuropsychology, Jagiellonian University, Institute of Applied Psychology, Krakow, Poland

[2]Department of Pharmacology, Laboratory of Pharmacology and Brain Biostructure, Maj Institute of Pharmacology, Polish Academy of Sciences, Krakow, Poland

[3]Department of Molecular Neuropharmacology, Maj Institute of Pharmacology, Polish Academy of Sciences, Krakow, Poland

Correspondence
Wojciech Solecki, Department of Neurobiology and Neuropsychology, Institute of Applied Psychology, Jagiellonian University, 4 Lojasiewicza Street, 30-348 Krakow, Poland.
Email: wojciech.solecki@uj.edu.pl

Funding information
Narodowe Centrum Nauki, Grant/Award Number: UMO-2018/29/B/NZ7/02672; Statutory funds of the Maj Institute of Pharmacology, Polish Academy of Sciences

Abstract

Noradrenergic neurotransmission is a critical mediator of stress responses. In turn, exposure to stress induces noradrenergic system adaptations, some of which are implicated in the etiology of stress-related disorders. Adrenergic receptors (ARs) in the ventral tegmental area (VTA) have been demonstrated to regulate phasic dopamine (DA) release in the forebrain, necessary for behavioral responses to conditional cues. However, the impact of stress on noradrenergic modulation of the VTA has not been previously explored. We demonstrate that ARs in the VTA regulate dopaminergic activity in the VTA–BLA (basolateral amygdala) circuit, a key system for processing stress-related stimuli; and that such control is altered by acute stress. We utilized fast-scan cyclic voltammetry to assess the effects of intra-VTA microinfusion of α_1-AR and α_2-AR antagonists (terazosin and RX-821002, respectively), on electrically evoked phasic DA release in the BLA in stress-naïve and stressed (unavoidable electric shocks – UES) anesthetized male Sprague–Dawley rats. In addition, we used western blotting to explore UES-induced alterations in AR protein level in the VTA. Intra-VTA terazosin or RX-821002 dose-dependently attenuated DA release in the BLA. Interestingly, UES decreased the effects of intra-VTA α_2-AR blockade on DA release (24 h but not 7 days after stress), while the effects of terazosin were unchanged. Despite changes in α_2-AR physiological function in the VTA, UES did not alter α_2-AR protein levels in either intracellular or membrane fractions. These findings demonstrate that NA-ergic modulation of the VTA–BLA circuit undergoes significant alterations in response to acute stress, with α_2-AR signaling indicated as a key target.

KEYWORDS
acute stress, dopamine, noradrenaline, ventral tegmental area, α_1-adrenergic receptor, α_2-adrenergic receptor

1 | INTRODUCTION

Maladaptive changes in the brain catecholamine – dopamine (DA) and noradrenaline (NA) – neurotransmitter systems are widely recognized to be implicated in conditions related to stress: affective disorders, anxiety disorders as well as substance use disorder (Aston-Jones & Harris, 2004; Koob, 2014; Koob et al., 2014; Morilak et al., 2005; Smith & Aston-Jones, 2008). Multiple neural hubs involved in affective, cognitive, and behavioral responses to acute stressors are also potentially relevant for subsequent development of anxiety-like behaviors. This includes, among others: regions of the medial prefrontal cortex (mPFC), lateral septum, the central and basolateral amygdala, bed nucleus of stria terminalis (BNST) and nucleus accumbens, NAc (Morilak et al., 2005). Here, the basolateral amygdala (BLA) is of special interest, as both DA and NA signaling converge in this structure (Sharp, 2017), regulating BLA function in fear conditioning as well as modulating anxiogenic effects of prolonged stress (Daviu et al., 2019; Giustino & Maren, 2018; Haubrich et al., 2020; Kwon et al., 2015; McCall et al., 2017; Sharp, 2017).

Among the neuroadaptations implicated in vulnerability to stress and anxiety, one stands out as particularly critical: dysregulation of catecholaminergic neurotransmission itself, which has the potential to engage a plethora of downstream mechanisms in multiple structures of interest due to the sheer volume and breadth of brain-wide NA- and DA-ergic innervation (Beier et al., 2015; Poulin et al., 2018; Schwarz & Luo, 2015). For instance, in the locus coeruleus (LC), stress elicits an overall increase in excitability and, presumably, NA production, through a number of alterations in intrinsic properties, morphology and receptor expression (Borodovitsyna, Flamini et al., 2018; Borodovitsyna, Joshi, et al., 2018). This is accompanied by similar changes in NA efferents. With the use of fast-scan cyclic voltammetry (FSCV) and similar techniques enabling the detection of catecholamine release with high-spatiotemporal precision, several groups have demonstrated that NA terminals in BNST and BLA respond to stressful stimuli or drug abstinence/withdrawal, often by decreasing NA uptake or dampening the regulatory action of α_2-adrenergic receptors, α_2-AR (Deal et al., 2021; Fox et al., 2015; McElligott et al., 2013; Schmidt et al., 2018). Both the reuptake of NA into terminals, as well as inhibition of its release via α_2-AR autoreceptors (Gilsbach & Hein, 2012), limit the availability and local extracellular spread of NA, determining its capability to engage α_1- and β-ARs. Thus, these changes in LC efferents can drive up the levels of NA and engage plasticity in target structures (Fox et al., 2017).

Dopaminergic neurons in the ventral tegmental area (VTA) also undergo changes in excitability in response to stress (Baik, 2020; Douma & de Kloet, 2020). Given the fact that the VTA receives adrenergic innervation from the LC as well as brainstem areas A1/A2 (Mejías-Aponte et al., 2009), and that ARs are known to be expressed on most of the compartments of the VTA, including DA neurons, GABA interneurons, afferents and glial cells (Mejias-Aponte, 2016), the VTA emerges as a potential important locus of NA-ergic modulation. In our previous study, we have shown that NA can act directly in the VTA, differentially influencing DA release in mesocortical and mesolimbic pathways. The release of DA in the mesolimbic pathway (from VTA to NAc core) was regulated by α_1-AR receptor antagonists infused into the VTA, in contrast to DA release in the mPFC (Kielbinski et al., 2019). In that study, we also found that intra-VTA administration of RX-821002, an α_2-AR antagonist, was capable of almost completely shutting down electrically-evoked phasic DA release in NAc and that dopamine D_2 receptors (D_2Rs) were required for this effect. We interpreted this finding as cross-activation of D_2R by high levels of NA released into the VTA in response to electrical stimulation coupled with acute α_2-AR autoreceptor blockade.

Given these priors: that BLA, an important structure involved in both fear and anxiety, is regulated by VTA DA-ergic input; that stressful stimuli have been demonstrated to decrease NA autoregulation by α_2-AR; and that intra-VTA infusion of α_2-AR antagonist results in attenuation of mesolimbic DA release, we asked whether the LC/A1/A2-VTA–BLA circuit exhibits stress-induced reduction in afferent α_2-AR regulation of NA release in the VTA after exposure to a stressful stimulus in the form of a series of unavoidable electric shocks (UES).

We used FSCV measurements of electrically evoked DA efflux in BLA to compare the effects of α_2-AR antagonist RX-821002 and α_1-AR antagonist terazosin in naïve rats and rats which had been subjected to UES 24 h prior to recording. We found that the effect of RX-821002, but not terazosin, was attenuated significantly by stress, suggesting that noradrenergic projections into the VTA exhibit reduced responses to α_2-AR autoregulation. These changes were transient, as 7 days after the exposure to electric shock the response to α_2-AR blockade was normalized to naïve levels. To probe for potential mechanisms of altered α_2-AR autoregulation, we performed the western blotting of VTA tissue samples treated with the protein crosslinker bissulfosuccinimidyl suberate (BS^3) to separate intracellular and membrane fractions. However, we detected no changes in α_{2A}-AR or D_2 dopamine receptor expression in either of these fractions in stressed animals compared to controls. Thus, stress-induced decrease in α_2-AR function is likely not mediated simply by changes in the expression or trafficking of α_2-AR and D_2 receptor proteins.

2 | MATERIALS AND METHODS

2.1 | Animals and study design

Adult male Crl:CD(SD) Sprague–Dawley rats (RRID:RGD_737891) weighing ~300 g at the start of the experiment were purchased from Charles River (Germany). Animals were housed in the Institute of Zoology and Biomedical Research, Jagiellonian University (Krakow, Poland). Animals were housed five per cage on a 12-hour light/dark cycle (lights on at 7 am – experimental procedures were performed during the light phase of the cycle), with ad libitum access to food and water and in a temperature- and humidity-controlled room. All the experimental procedures were conducted according to the EU Guide for the Care and Use of Laboratory Animals and were approved by the Committee on

the Ethics of Animal Experiments at the Institute of Pharmacology, Polish Academy of Sciences, Krakow, Poland (approval n. 165/2019). The study was not pre-registered. Due to the within-subject design limiting the bias introduced by control vs treatment allocation, subjects were allocated to treatments non-randomly on a cohort-by-cohort basis. No blinding was performed during FSCV experiments due to practical limitations, histological evaluation post-experiment was blinded (subjects coded by date and decoded after verification).

2.2 | Drugs

Terazosin (α_1-AR antagonist, 5 μg, final concentration of 25.8 mM; cat. n. T4680, Sigma Aldrich, Germany), RX-821002 (α_2-AR antagonist, 2.7 μg or 13.5 μg, final concentration of 23.06 mM, and 115.26 mM; cat. n. 1324, Tocris Bioscience, United Kingdom) were dissolved in sterile 0.9% saline and administered in a total volume of 0.5 μl via a micropump (53 127 V, Stoelting Europe, Ireland) driving a 10 μl syringe (26 s ga, Hamilton 701 N).

The injection of the drug into the structure was performed for 1 min, then the internal cannula was left at the injection site for another 1 min for complete diffusion into the tissue. The doses used were derived from previous studies (Kielbinski et al., 2019; Park et al., 2017).

2.3 | Unavoidable electric shock

Prior to FSCV or tissue preparation for western blot, rats from the experimental group were subjected to a series of unavoidable electric shock. Each rat was placed in the experimental chamber with a metal grid floor, one opaque Plexiglas sidewall, three metal sidewalls, a 24-V house light located on the opaque Plexiglas ceiling, and a white stimulus lamp illuminated by a 24-V bulb and a tone generator, both located on a metal sidewall. At 180 s, after being placed in the experimental chamber, all rats received four series of electric shocks, each consisting of a 30-s tone (60 dB) and light presentation co-terminated with a 2 s 0.9 mA electric footshock. The inter-trial interval lasted 60 s. 24 h or 7 days after the UES procedure animals were subjected to FSCV experiments.

2.4 | Surgical procedures

Animals were deeply anesthetized with urethane (1.5 g/kg i.p.; cat. n. U2500, Sigma Aldrich) and maintained under full anesthesia throught the experiment, followed by immediate sacrifice (nonrecovery procedure). Urethane is a general anesthetic routinely used in electryphysiological and electrochemical in vivo studies, characterized by long-lasting (up to 24 h) and stable anesthesia and analgesia (Field et al., 1993). The depth on anesthesia was monitored throughout, no cases of premature termination of the

procedure due to loss of anesthesia were encountered. A heating pad was used throughout all experimental procedures to avoid hypothermia.

Animals were secured in a stereotaxic frame (Stoelting Europe, Ireland), the skin and tissue were removed to expose the skull and the bregma reference point was identified (Paxinos & Watson, 2013). Holes were then drilled, using bregma as a reference for the stimulation and recording electrodes. A carbon-fiber microelectrode consisting of a glass capillary (A-M, standard 1 mm diameter) and carbon fiber (7 μm carbon diameter, cut to 50–80 μm) was inserted into the basolateral amygdala at the following coordinates (anteroposterior, mediolateral and dorsoventral displacement in mm from bregma): AP -2.0 to −2.4; ML +4.6; DV -7.1 to −7.4 below the dura. The bipolar stainless steel stimulating electrode combined with a guide cannula (1 mm width, 26 ga guide; Plastics One) was placed in the VTA: AP -5.3 to −5.5, ML −1.0, DV from dura-7.9 to −8.3. A reference Ag/AgCl electrode was inserted into the contralateral hemisphere and secured tightly with a single screw.

2.5 | Histological verification

At the end of each experimental session, a lesion was made at the recording site by stepwise application of current from 6 to 10 μA, then animals were decapitated and brains were preserved in 10% formalin for later sectioning into 100 μm coronal slices (on a Leica VT-1000S vibratome) for histological verification of stimulation and recording electrode placements. Implantation sites of both recording and stimulating electrodes were verified using a light microscope. Only animals where both the recording and stimulation electrodes were placed unambiguously in the BLA and VTA, respectively, based on corresponding anatomical sections in the rat brain atlas (Paxinos & Watson, 2013) were included. Figure S1 shows implantation sites of stimulating electrodes (VTA) and recording electrodes (BLA).

2.6 | Fast-scan cyclic voltammetry (FSCV)

The FSCV measurements were performed with techniques and equipment described previously (Kielbinski et al., 2019).

Briefly, the system consisted of a custom-built controller and headstage (University of North Carolina Department of Chemistry, Electronics Facility, Chapel Hill, USA) as well as stimulus isolator (DS 4, Digitimer Ltd) under the control of HDCV software (UNC Dept. of Chemistry Electronics Facility, Chapel Hill, USA).

A triangular waveform (from −0.4 V to +1.3 V against the Ag/AgCl reference, at a scan rate of 400 V/s applied in 850 steps of 2 mV per 100 ms window) was applied to the recording site. Background-subtracted, low-pass filtered (2 kHz) signal was used to generate cyclic voltammograms. Recordings were obtained as described previously (Kielbinski et al., 2019). For evoking DA release, the VTA was stimulated with a biphasic square waveform (300 μA; 2 ms per phase; 24 pulses) with 60 Hz frequency corresponding to "phasic"

activity. Each trace consisted of 15 s of recording, with stimulation being performed at $t = 5$ s.

The experimental design is shown in Figure 1 and consisted of measurements performed at baseline, followed by a control infusion of saline into the VTA, followed by another, second baseline measurement, after which drug infusion was performed. For each condition, 5 to 6 consecutive measurements were taken, 180 s apart, to allow the local environment to equilibrate through DA uptake and to restore DA stores in neuronal terminals at the recording site (Wickham et al., 2013).

2.7 | Tissue preparation

For tissue preparation (previously described in Bator et al., 2018; Boudreau & Wolf, 2005; Chocyk et al., 2013), animals – naïve or 24 h post-UES – were killed by decapitation, the brains were immediately removed from the skull and dissected. Samples of the VTA were obtained with a small biopsy punch, then minced with a scalpel blade. The tissue was then transferred to tubes filled with cold ACSF (containing in mM: 118 NaCl, 25 $NaHCO_3$, 3 KCl, 1.2 NaH_2PO_4, 2 $CaCl_2$, 1.3 $MgSO_4$, 10 glucose) and 5 mM bissulfosuccinimidyl suberate (BS^3; cat. n. 21 580, Thermo Scientific) solution was added. Crosslinker BS^3 is a water-soluble analogue of N-hydroxysuccinimide ester that reacts efficiently with primary amino groups (–NH2) of proteins to form stable amide bonds. Furthermore, BS^3 cannot pass through the cell membrane and binds only to fragments protruding from the

membrane, forming cross-linked protein complexes, while having no effect on intracellular proteins. The use of the BS^3 crosslinker thus allows the separation of proteins on the cell surface from intracellular proteins in the same sample without prior fractionation (Boudreau et al., 2012). Tissue samples in ACSF–BS^3 solution were incubated for 30 min on ice with gentle agitation. The reaction was terminated by adding 20 mM glycine (Sigma Aldrich) followed by a 10 min incubation on ice. Then, the samples were pelleted by brief centrifugation, the supernatant was discarded and the pellet was resuspended in cold lysis buffer (PathScan® Sandwich ELISA Lysis Buffer [1X], Cell Signaling) with protease and phosphatase inhibitor cocktails (1:200; Sigma) and homogenized (TissueLyser, Retsch). The total protein concentrations in the extracts were determined using the QuantiPro BCA Assay kit (Sigma).

2.8 | Western blotting

Samples with an equal amount of protein extract (for α_{2A}-AR protein, 40 μg; and for D_2R protein, 30 μg of protein per lane) were separated using 7.5% SDS–PAGE and transferred onto a nitrocellulose membrane using an electrophoretic transfer system (Bio-Rad). Then the membranes were incubated overnight at 4°C with the following primary antibodies: rabbit anti-ADRA2A (1:500; cat. n. NBP2-22452, NovusBio) or rabbit anti-DRD2 (1:1000; RRID:AB_2094980, cat. n. AB5084P, Millipore) and rabbit anti-GAPDH (1:5000; cat. n. 14C10 2118S, Cell Signaling Technology). A suitable secondary antibody
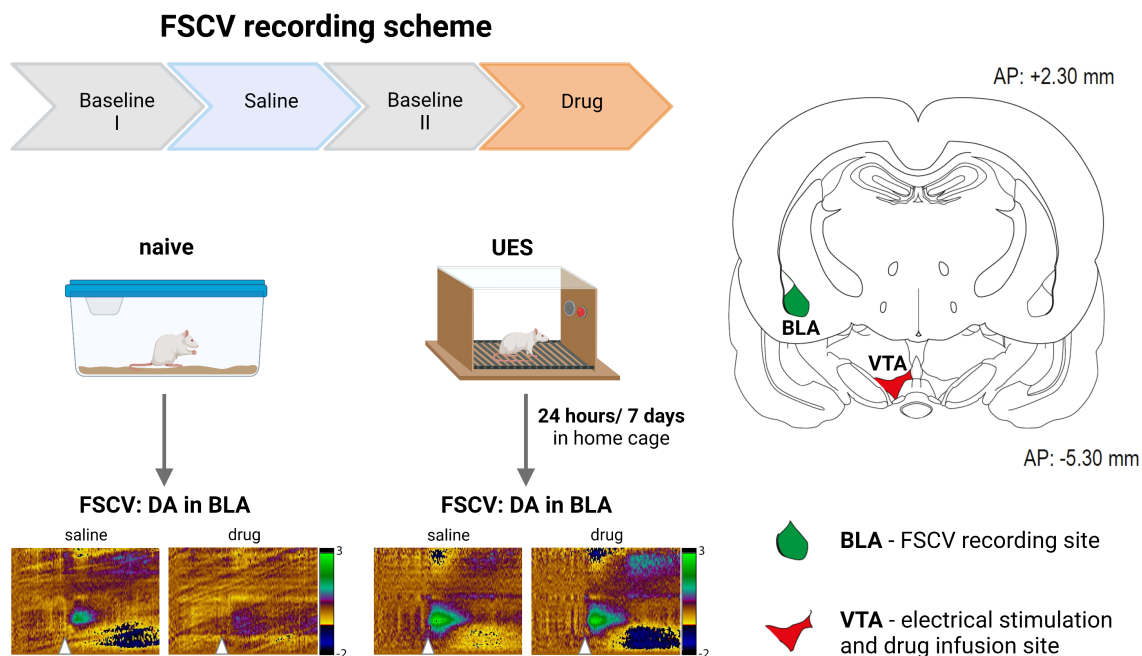

FIGURE 1 Schematic of the FSCV experiment. Top: Experimental design. Each stage consisted of a series of recordings: Baseline, followed by an injection of saline into the VTA and a series of "saline" recordings, followed by a baseline series ("baseline II"), followed by drug administration and recording. Bottom: The experiment included a "naïve" control group and the "UES" experimental groups which underwent unavoidable electric shock procedure 24 h or 7 days before the FSCV experiment; shown are examples of color plots of electrically evoked DA in BLA after VTA stimulation (white triangles). Right: Schematic coronal sections from the brain atlas (Paxinos & Watson, 2013), showing recording site in the BLA (green) and electrical stimulation and infusion site in the VTA (red).

was used to detect immune complexes (rabbit IgG antibody, 1:1000 from Lumi-Light^{PLUS} Western Blotting Kit, cat. n. 12015 218001, Roche – incubation for 1 h at room temperature). The reactions were visualized with enhanced chemiluminescence (ECL; Lumi-Light^{PLUS} Western Blotting Kit, Roche). Chemiluminescence was imaged using a luminescent image analyzer (Fujifilm LAS-1000; Fujifilm Corporation). Relative immunoreactivity levels for α_{2A}-AR and GAPDH proteins were quantified using ImageJ software (Schneider et al., 2012). Density of the BS^3-conjugated and unconjugated fractions were then expressed as ratios of α_{2A}-AR/GAPDH and expressed as Z-scores to facilitate comparisons between technical replicates (blots).

2.9 | Data analysis

The HDCV Analysis software (UNC Department of Chemistry Electronics Facility, Chapel Hill, NC, USA) was used to quantify relative changes in phasic DA efflux as described previously (Kielbinski et al., 2019). Briefly, representative traces of electrically evoked phasic DA were obtained in vivo at different stimulation parameters (combinations of 12, 24, 48 pulses at stimulation amplitude of 200, 300, and 400 μA, resulting in outputs spanning the range of signals expected under experimental conditions) and used as training sets for principal component regression analysis using the HDCV software's built-in capabilities (Bucher et al., 2013; Keithley & Wightman, 2011; Rodeberg et al., 2015). Components corresponding to DA and pH were identified and peak values corresponding to phasic DA were either averaged per experimental condition or used separately to study changes over time. In all cases, DA levels after saline or antagonist intra-VTA administration were expressed as percentile ratios representing change in DA efflux versus the average of their respective 5–6 baseline traces (Figure 1). Additionally, the difference of % DA changes after saline vs drug injection was calculated to compare the respective effects in naïve and stressed subjects.

Only datasets meeting minimal quality criteria – stable baseline DA levels (i.e., distinctly identifiable, upon visual inspection, peaks corresponding to stimulation, with no non-stimulated peaks or fluctuation at a similar amplitude), no missing measurements (for time-course data; for averaged values, data sets of at least 4 traces with no consecutive rejected traces were accepted) and no contamination from above-background residual signal in PCA output – were included in the final analysis. Initial numbers of subjects used were determined based on similar previously published experiments (Kielbinski et al., 2019); the effect of terazosin on NAc phasic DA was taken as a conservative estimate of an expected effect – post-hoc power analysis for repeated-measures T-test on this data (observed standardized difference $d = 1.544588$) yielded power>0.85 for $n \geq 6$, assuming two-sided $p = 0.05$.

Summary of animals used and excluded from the experiments on the basis of histological verification or failure of the recorded data to meet quality criteria is shown in Table 1.

Relative changes in phasic DA after saline and drug infusion were compared with repeated measures T-tests (for average effect calculation), or with repeated measures two-way analysis of variance (RM ANOVA) for time course data, with within-subjects drug treatment and time effects as well as drug-time interaction. For differences between saline and drug changes, simple (unpaired) T-tests or ANOVA were used, with drug dose and treatment (naïve vs UES), where appropriate. For normalized relative levels of α_{2A}-AR signal obtained from western blotting, unpaired T-tests were used as well. In all cases, $p < 0.05$ (two-sided) was taken as the threshold of significance. No outlier removal or value imputation methods were used; data conformation towards parametric statistical test assumptions was verified by histogram and residual plot evaluation. All the statistical analyses were performed with Prism 9.0 (GraphPad Software).

3 | RESULTS

3.1 | Intra-VTA α_1-AR antagonist terazosin reduces DA release into the BLA but is not modulated by a single episode of UES

After administration of the α_1-AR antagonist terazosin (5 μg) to the VTA, we observed a significant decrease in the average level of electrically evoked phasic DA released into the BLA in comparison with saline control (Figure 2b; paired T-test $t_{[6]} = 3.71$, $n = 7$ rats, $p = 0.01$). The results obtained in animals after a single episode of UES are analogous to those in naïve animals, i.e., intra-VTA terazosin (5 μg) causes a reduction in average DA levels in the BLA (Figure 2e; paired T-test $t_{[7]} = 3.79$, $n = 8$ rats, $p = 0.0068$). Time comparisons of single traces showed no significant effect of terazosin administration at a dose of 5 μg in both naïve (Figure 2c; RM ANOVA: drug effect $F_{(1,4)} = 7.691$, $n = 5$ rats, $p = 0.0502$; time effect $F_{(2.338,9.353)} = 1.357$, $n = 5$, $p = 0.31$; time x drug $F_{(2.869,11.48)} = 0.4284$, $n = 5$, $p = 0.73$) and stressed rats (Figure 2f; RM ANOVA: drug effect $F_{(1,4)} = 5.016$, $n = 5$ rats, $p = 0.089$; time effect $F_{(2.014,8.057)} = 0.3247$, $n = 5$, $p = 0.73$; time x drug $F_{(1.961,7.846)} = 2.25$, $n = 5$, $p = 0.17$). Moreover, a direct comparison of saline-drug differences in relative DA change from baseline between the naïve and UES groups showed no difference in the effect induced by intra-VTA administration of terazosin (Figure 5a; unpaired T-test $t_{[13]} = 0.31$, $n = 14$, $p = 0.76$).

3.2 | Intra-VTA α_2-AR antagonist dose-dependently reduces electrically evoked phasic DA release into the BLA

Administration of an α_2-AR antagonist (RX-821002) at a dose of 2.7 μg to VTA resulted in a decrease in electrically evoked, phasic DA release into the BLA in naïve animals (Figure 3b; paired T-test $t_{[5]} = 7.64$, $n = 6$ rats, $p = 0.0006$). Furthermore, administration of a higher dose of RX-821002, i.e., 13.5 μg resulted in nearly complete blockade of DA release into the BLA (Figure 3e; paired T-test

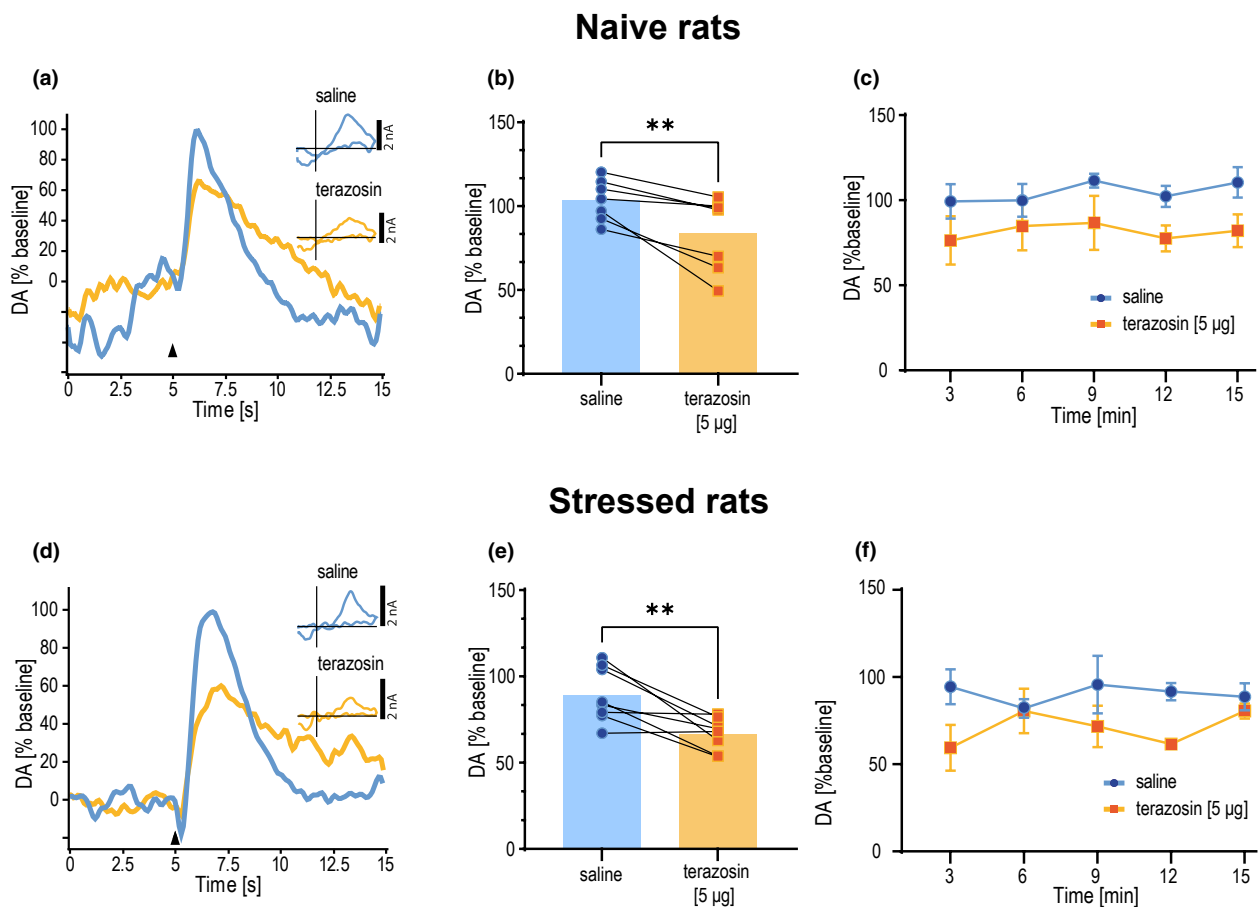| Drug	Initial	Excluded (data quality)	Excluded (histological verification)	Final n
Terazosin 5.0 μg naïve	9	0	2	7
Terazosin 5.0 μg stressed	12	1	3	8
RX-821002 2.7 μg naïve	8	1	1	6
RX-821002 2.7 μg stressed	9	0	3	6
RX-821002 13.5 μg naïve	8	0	2	6
RX-821002 13.5 μg stressed	9	1	1	7
RX-821002 13.5 μg 7 days after stress	8	0	3	5

FIGURE 2 Effects of terazosin intra-VTA infusion on electrically evoked phasic DA release in the BLA in naïve and stressed animals. (a, d) Representative FSCV traces obtained after infusion of saline and terazosin (5 μg) in naïve (a) and stressed (d) rats. Insets show representative current to voltage traces obtained from BLA in response to VTA stimulation after saline and terazosin. (b, e) plots of averaged DA values, bars represent the average obtained from all results, points represent individual measurements in naïve (b, $n = 7$) and stressed (e, $n = 8$) rats. **$p < 0.01$ in paired Student's test. (c, f) time course comparisons of relative DA peaks (% of their corresponding baseline) over five consecutive measurements in naïve ($n = 5$) and stressed ($n = 5$) rats after saline and terazosin (5 μg).

$t_{[5]} = 7.52$, $n = 6$ rats, $p = 0.0007$). Time comparisons of single traces showed a significant effect of RX-821002 at both doses. For 2.7 μg (Figure 3c; RM ANOVA: drug effect $F_{(1,4)} = 70.62$, $n = 5$ rats, $p = 0.0011$; time effect $F_{(1.479,5.917)} = 0.6732$, $n = 5$, $p = 0.50$; time x drug $F_{(1.634,6.537)} = 0.6613$, $n = 5$, $p = 0.52$) Sidak's post-test of multiple comparisons showed significant differences for

three initial time points (i.e. 3, 6, 9 min.). For the 13.5 μg dose (Figure 3f; RM ANOVA: drug effect $F_{(1,4)} = 38.81$, $n = 5$ rats, $p = 0.0034$; time effect $F_{(1.942,7.766)} = 3.163$, $n = 5$, $p = 0.10$; time x drug $F_{(2.035,8.140)} = 0.4145$, $n = 5$, $p = 0.68$) Sidak's multiple comparisons post-test revealed significant differences for first four time points (3–12 min).

3.3 | UES decreases the effects of intra-VTA administration of RX-821002 in BLA

A single episode of UES resulted in a complete blockade of the effect that was induced by intra-VTA administration of a low (2.7 µg) dose of RX-821002 in naïve animals. In stressed animals, the average DA levels obtained after saline and RX-821002 (2.7 µg) were not different from saline control (Figure 3h; paired T-test $t_{[5]} = 0.88$, $n = 6$ rats, $p = 0.42$). Comparison of individual time points also showed no significant differences (Figure 3i; RM ANOVA: drug effect $F_{(1,5)} = 4.582$, $n = 6$ rats, $p = 0.085$; time effect $F_{(1.92,9.962)} = 0.7583$, $n = 6$, $p = 0.49$; time x drug $F_{(1.852,9.258)} = 0.8399$, $n = 6$, $p = 0.45$).

In contrast, in animals that underwent a single episode of UES, administration of a high dose of an α_2-AR antagonist (RX-821002, 13.5 µg) to the VTA reduced the average level of DA release to the BLA, but to a lesser extent than in naïve animals (Figure 3l paired T-test $t_{[6]} = 4.55$, $n = 7$ rats, $p = 0.0039$). Similarly, comparisons based on single trace time points showed a significant effect (Figure 3m; RM ANOVA: drug effect $F_{(1,5)} = 10.18$, $n = 6$ rats, $p = 0.024$; time effect $F_{(1.662,8.311)} = 1.033$, $n = 6$, $p = 0.38$; time x drug $F_{(2.318,11.59)} = 0.4904$, $n = 6$, $p = 0.65$), however, none of the particular time-point comparisons reached significance based on Sidak's multiple comparisons tests. In addition, a direct comparison of the effects induced by the administration of two doses of RX-0821002 in naïve and stressed animals showed a significant main effect of treatment (Figure 5b; two-way ANOVA; $F_{(1,21)} = 20.92$; $p = 0.0002$), multiple comparisons test revealed differences between the naïve and UES groups after the administration of 2.7 µg RX-821002 ($p = 0.0003$), and 13.5 µg RX-821002 ($p = 0.0466$).

3.4 | Seven days after a single episode of UES, the effects of RX-821002 administration were normalized

Given the clear effects of a single episode of UES on the modulation of DA release in the BLA by α_2-AR blockade in the VTA, we next set out to test how long this change would persist. To this end, we performed FSCV experiments 7 days after the UES procedure. Interestingly, the results obtained 7 days after UES were similar to those observed in naïve animals, with the average DA level in BLA decreased significantly after intra-VTA RX-821002 (2.7 µg) administration (Figure 4b; paired T-test $t_{[4]} = 6.15$, $n = 5$ rats, $p = 0.0035$). In addition, comparisons of single traces over time showed a significant effect of RX-821002 intra-VTA infusion (Figure 4c; RM ANOVA: drug effect $F_{(1,4)} = 40.60$, $n = 5$, $p = 0.0031$; time effect $F_{(1.485,5.938)} = 0.4542$, $n = 5$, $p = 0.60$; time x drug $F_{(2.670,10.68)} = 2.149$, $n = 5$, $p = 0.16$). Significant decreases in DA release were found at 4 of the 6 time points (3, 9, 12, 15 min) based on Sidak's multiple comparisons post-test. A direct comparison between the groups: naïve, 24 h and 7 days after UES showed a significant, but transient effect of stress on the level of DA released into the BLA (Figure 5c, one-way ANOVA; $F_{(2,14)} = 9.86$; $p = 0.0021$). Tukey's multiple comparisons test revealed significant differences

between the naïve and 24 h post-UES ($p = 0.0028$), as well as 24 h post-UES and 7 days post-UES groups ($p = 0.01$), while the naïve and 7 days post-UES groups did not differ ($p = 0.88$).

3.5 | Protein levels of either the membrane or intracellular fractions of both α_2 and D_2 receptors are not modulated by a single episode of UES

Given our results showing that a single episode of UES affects α_2 receptor-dependent modulation of DA release in the BLA, and data from our previous work showing that D_2 receptors are required for the effect induced by intra-VTA administration of an α_2-AR antagonist (Kielbinski et al., 2019), we decided to test whether protein levels of both of these receptors (α_{2A}-AR and D_2R) change following UES. Both a band with a predicted molecular mass of approximately 50–70 kDa, corresponding to α_{2A}-AR or D_2R (intracellular protein) and a band with a high molecular mass (corresponding to BS^3-crosslinked α_{2A}-AR or D_2R membrane-expressed protein) were observed in BS^3-treated tissues prepared from VTA samples of both naïve animals and rats subjected to a single episode of UES. We then compared the standard scores between control and stressed groups in terms of membrane protein levels, intracellular protein levels and the ratio of these fractions to each other. UES had no effect on membrane α_{2A}-AR protein levels (Figure 6b; unpaired T-test $t_{[14]} = 0.28$, $p = 0.78$), intracellular levels (Figure 6c; unpaired T-test $t_{[14]} = 0.79$, $p = 0.44$) and the ratio of membrane to intracellular levels (Figure 6e; unpaired T-test $t_{[14]} = 0.90$, $p = 0.38$).

As with α_{2A}-AR protein levels, a single episode of UES did not affect D_2R protein expression in either of the fractions studied, i.e., membrane (Figure 6f; unpaired T-test $t_{[15]} = 0.53$, $p = 0.60$) and intracellular (Figure 6g; unpaired T-test $t_{[15]} = 0.22$, $p = 0.83$), and there were no statistically significant differences in the ratio of membrane to intracellular D_2R protein levels (Figure 6h; unpaired T-test $t_{[15]} = 0.29$, $p = 0.78$; unpaired T-test $t_{(15)} = 0.29$, $p = 0.78$).

4 | DISCUSSION

4.1 | Regulation of BLA DA release by NA input to the VTA

Owing to its wide reciprocal connectivity, BLA is well-positioned to influence both positive and negative valence attribution and consequent processing of stimuli in the short term, as well as network-level changes in emotional processing that gives rise to anxiety-like behavior in the longer term (Daviu et al., 2019; Janak & Tye, 2015). These functions are modulated by both NA- and DA-ergic inputs (de la Mora et al., 2010; Giustino & Maren, 2018; Janak & Tye, 2015; Lee et al., 2017; Sharp, 2017; Stubbendorff & Stevenson, 2021). Optogenetic experiments have shown that NA can modulate BLA directly, via β-ARs (McCall et al., 2015),

Naive rats
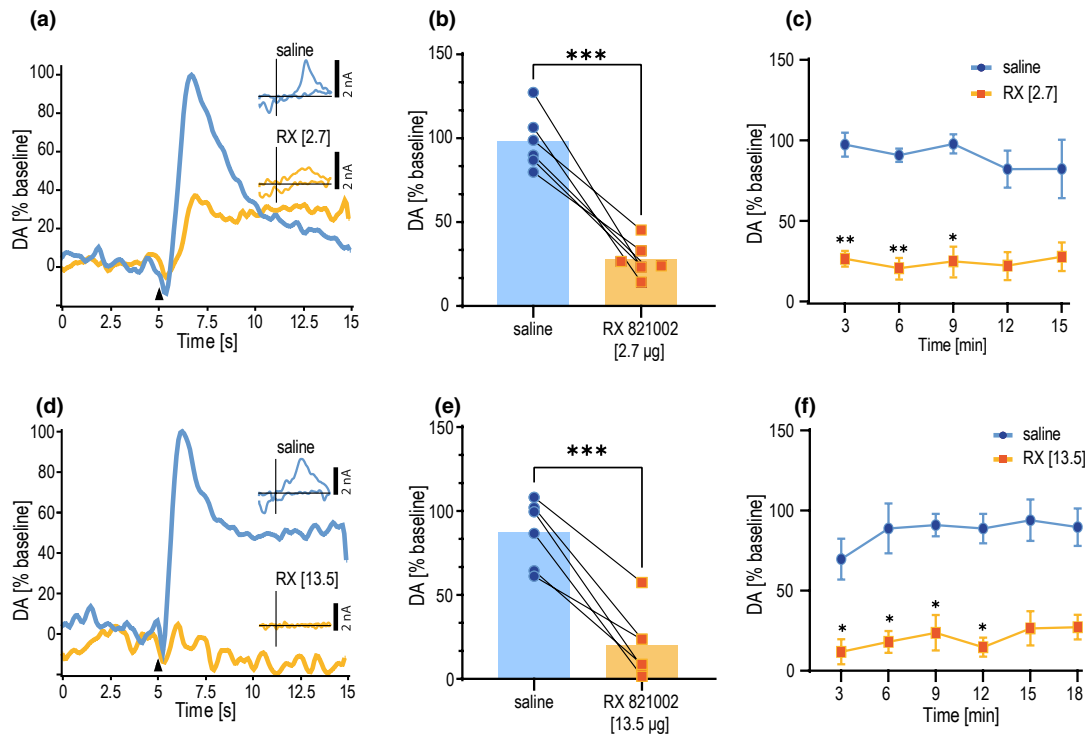
Stressed rats
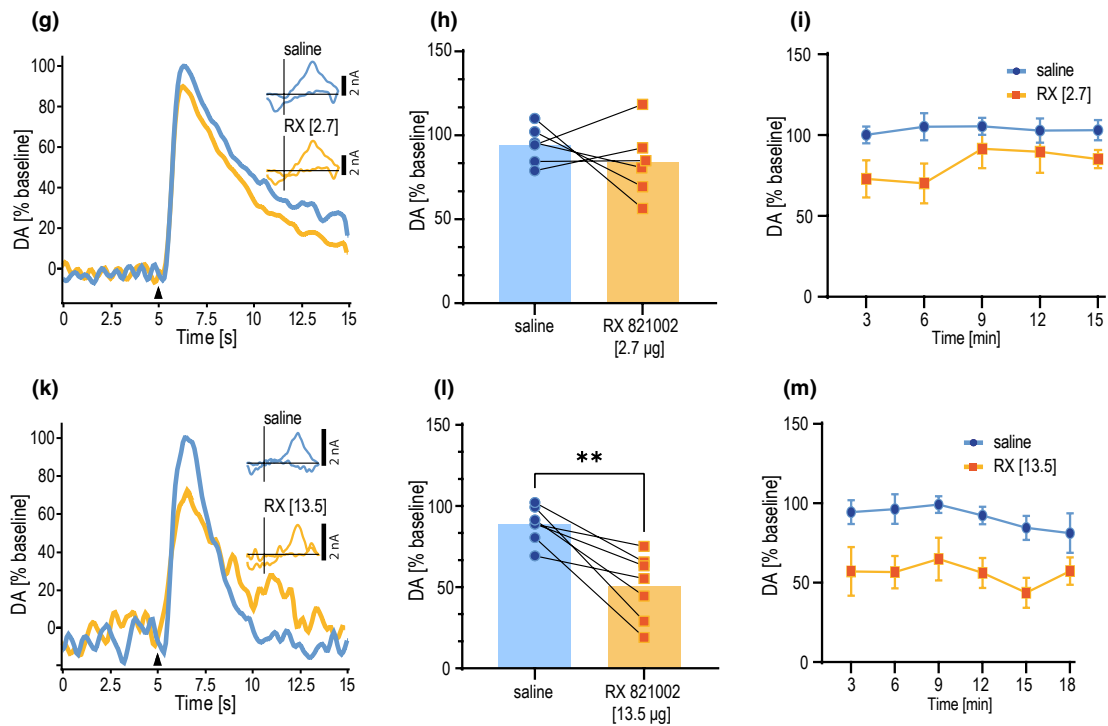
however, it was previously unclear whether activation of the NA system is capable of modulating the DA-ergic input into BLA as well – a hypothesis made likely by the observation that intra-VTA administration of AR antagonists modulates conditioned behaviors in which BLA is involved (Solecki et al., 2017, 2018, 2019).

In the present study, we report that – similarly to projections from the VTA to NAc and in contrast to projections into mPFC (Kielbinski et al., 2019) – DA neurons projecting to BLA are also recruited from a pool of cells that respond to NA via both α_1-AR- and D_2R-mediated regulation. In contrast to DA projections from the

FIGURE 3 Effects of RX-821002 intra-VTA infusion on electrically evoked phasic DA release in the BLA in naïve and stressed animals. (a, d) representative FSCV traces obtained after infusion of saline and 2.7 µg (a) and 13.5 µg (d) RX-821002 in naïve rats. Insets show representative current to voltage traces obtained from BLA in response to VTA stimulation after saline and RX-821002. (b, e) plots of averaged DA values, bars represent the average obtained from all results, points represent individual measurements after administration of saline and RX-821002 at doses of 2.7 µg (b, $n = 6$) and 13.5 µg (e, $n = 6$) in naïve rats. ***$p < 0.001$ in paired Student's test. (c, f) time course comparisons of relative DA peaks (% of their corresponding baseline) over six consecutive measurements in naïve rats after saline and RX-821002 (c: 2.7 µg, $n = 5$ and f: 13.5 µg, $n = 5$). *$p < 0.05$, **$p < 0.01$, ***$p < 0.001$ in Sidak multiple comparisons post-hoc test. (g, k) representative FSCV traces obtained after infusion of saline and 2.7 µg (g) and 13.5 µg (k) RX-821002 in stressed rats. (h, l) plots of averaged DA values after administration of saline and RX-821002 at doses of 2.7 µg (h, $n = 6$) and 13.5 µg (l, $n = 7$) in stressed rats. **$p < 0.01$ in paired Student's test. (i, m) time course comparisons of relative DA peaks (% of their corresponding baseline) over six consecutive measurements in stressed rats after saline and RX – 821002 (i: 2.7 µg, $n = 6$ and 13.5 µg, $n = 6$: M). *$p < 0.05$ in Sidak multiple comparisons post-hoc test.
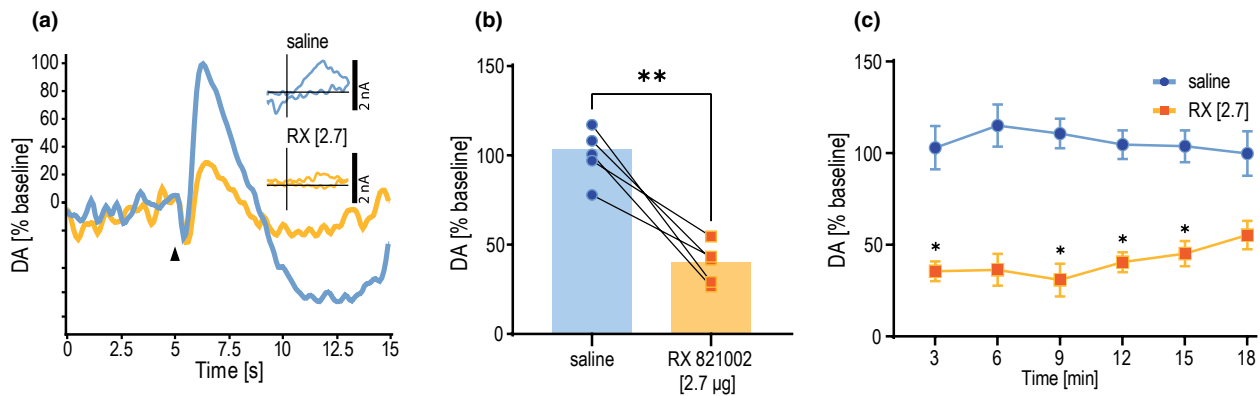

FIGURE 4 Effects of RX-821002 intra-VTA infusion on electrically evoked phasic DA release in the BLA in rats 7 days after UES. (a) Representative FSCV traces obtained after infusion of saline and RX-821002 (2.7 µg) in rats at 7 days post-UES. Insets show representative current to voltage traces obtained from BLA in response to VTA stimulation after saline and RX-821002. (b, $n = 5$) plots of averaged DA values, bars represent the means, points represent individual measurements after administration of saline and RX-821002 (2.7 µg). **$p < 0.01$ in paired Student's test. (c, $n = 5$) time course comparisons of relative DA peaks (% of their corresponding baseline) over six consecutive measurements in rats after saline and RX-821002 (2.7 µg). *$p < 0.05$, **$p < 0.01$ in Sidak multiple comparisons post-hoc test.

VTA to dorsal and ventral striatum, the VTA–mPFC and VTA–BLA pathways are seldom studied with voltammetric tools, owing to relative technical difficulty – both due to lower DA output, and the fact that these structures receive NA- as well as DA-ergic innervation, which could potentially introduce issues with interpretation of the voltammetric signal. Nonetheless, based on anatomical and pharmacological characterization, stimulation of the VTA indeed seems to specifically elicit DA release with no evidence of mixed catecholamine (DA/NA) output in those areas (Garris et al., 1994; Holloway et al., 2019; Shnitko & Robinson, 2014). The kinetics of electrically evoked VTA-BLA DA are consistent with a much smaller available neurotransmitter pool and thus significantly lower peak release, as well as slower uptake via transporters compared to striatal DA (Garris et al., 1994; Holloway et al., 2019), in line with postulated broader diffusion and neuromodulatory action at this site.

A large anatomical study (Poulin et al., 2018) has previously explored the projection sites of several populations of tyrosine hydroxylase-positive VTA DA neurons defined with intersectional transgenic tools in mice. The predominant population innervating NAc core – cholecystokinin-positive (Cck+) neurons – also densely innervates BLA. In contrast, the comparatively sparse innervation in the prefrontal cortex consists primarily of Vglut-positive neurons,

with a small admixture of Cck+. Thus, we presume that these Cck + cells constitute the common molecular subtype of DA neurons projecting to both BLA and NAc that is responsive to modulation by NA. It is still unclear, however, whether these projections are subserved by the same neurons, and their specialization (responsible for differences in DA release and uptake) is limited to NAc and BLA terminals, or if these are separate cells sharing some molecular characteristics.

4.2 | Mechanisms of α_1-AR and α_2-AR regulation of VTA

In the VTA, the α_1-AR antagonist terazosin could reduce evoked DA through a variety of candidate mechanisms: direct postsynaptic modulation of cell excitability (Goertz et al., 2015), regulation of neurotransmitter release at local glutamatergic and GABA terminals (Velásquez-Martinez et al., 2020, 2012, 2015) and interaction with other receptors (Paladini et al., 2001; Tovar-Díaz et al., 2018; Williams et al., 2014). When infused into the VTA, the α_2-AR antagonist RX-821002, in line with our previous findings in NAc core, potently inhibits electrically evoked DA release in BLA, likely by a mechanism involving cross-activation of D_2 receptors
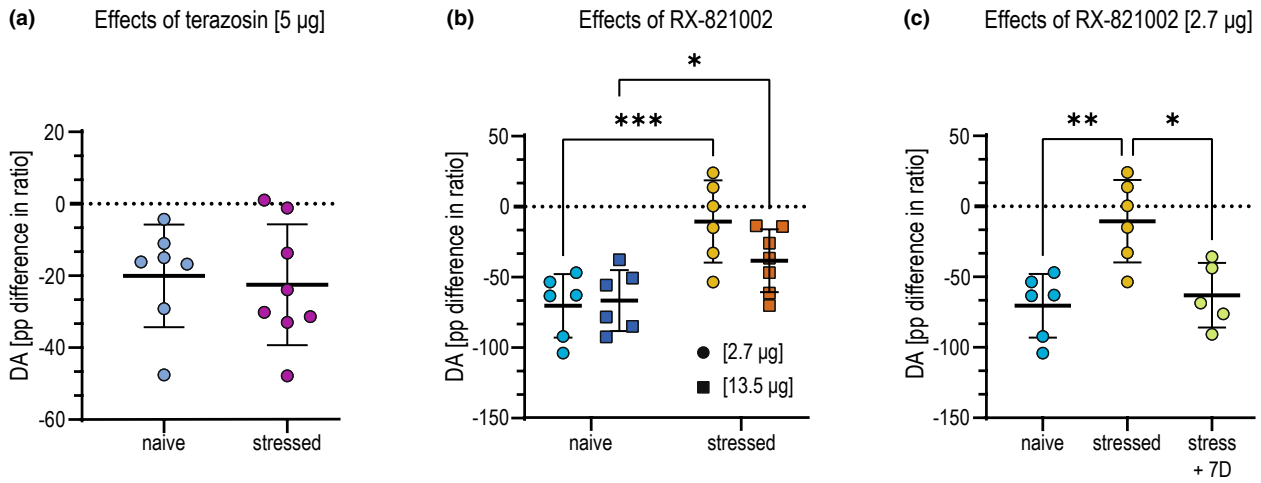
FIGURE 5 Comparisons of average effects of terazosin and RX-821002 intra-VTA administration in stressed and naïve animals. (a) Difference in average relative DA values (saline – Terazosin) in naïve rats ($n = 7$) and animals 24 h post-UES ($n = 8$). (b) Difference in average relative DA values (saline – RX-821002) after 2.7 μg and 13.5 μg RX-821002 intra-VTA infusion in naïve ($n = 6$; $n = 6$, respectively) and 24 h post-UES groups ($n = 6$; $n = 7$, respectively). (c) Difference in average relative DA values (saline – RX-821002) after 2.7 μg RX-821002 intra-VTA infusion in naïve ($n = 6$), 24 h post-UES ($n = 6$) and 7 days post-UES ($n = 5$). Differences expressed as percentage points (saline – Drug). $^*p < 0.05$, $^{**}p < 0.01$, $^{***}p < 0.001$ in multiple comparisons post-hoc tests.
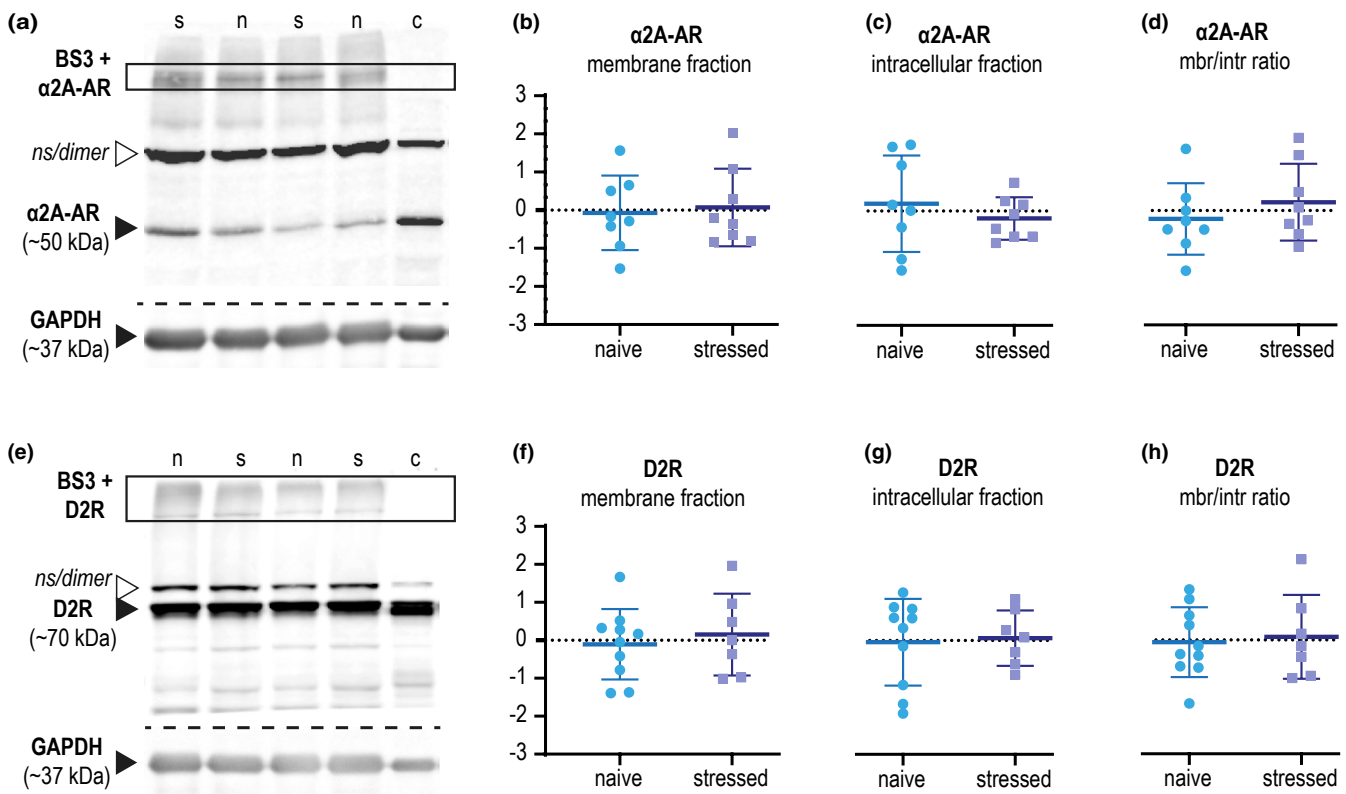

FIGURE 6 Effect of a single episode of UES on α_{2A}-AR and D_2R protein levels in rat VTA - western blot analysis. Representative immunoblots probed with antibodies for (a) α_{2A}-AR and (e) D_2R and GAPDH. Membrane (b, f), intracellular (c, g) and ratio of membrane to intracellular protein levels (d, h) of α_{2A}-AR and D_2R protein, respectively, in control ($n = 8$ and $n = 10$ for α_{2A}-AR and D_2R respectively) and stressed ($n = 8$; $n = 9$) groups. Plots show mean Z-score values with standard deviation, points show single measurements.

by NA (Arencibia-Albite et al., 2007; Grenhoff et al., 1995). This is corroborated by studies showing that D_2-like receptors have a relatively similar affinity towards NA and DA and that NA binding to these receptors is indeed capable of activating G-protein dependent downstream signaling (Guiard et al., 2008; Sánchez-Soto et al., 2016). In addition, (Park et al., 2017) have observed

that while electrical stimulation of LC evoked putative DA release in NAc, systemic administration of the α_2-AR antagonist idazoxan inhibited NAc catecholamine release.

4.3 | Attenuated α_2-AR autoreceptor control over VTA NA after stress

The second major finding here is that, following a single episode of acute stress in the form of UES, the effects of RX-821002 were significantly reduced. The efficacy of the larger dose used in the study (13.5 µg per infusion) was significantly decreased, while the 2.7 µg dose, which in naïve animals was effective at reducing electrically evoked DA, had no effect. This change in responsivity to α_2-AR antagonist was transient, as 7 days after exposure to stress, normalized responses to intra-VTA RX-821002 were observed. This observation fits within the body of data reported previously in other NA release sites, particularly BNST (Fox et al., 2015; McElligott et al., 2013; Schmidt et al., 2018). Using similar techniques of voltammetry and pharmacological challenge, these authors initially reported that the releasable pool of NA in BNST terminals, its uptake, as well as regulation by α_2-ARs, was altered by either baseline susceptibility to stress in rat lines bred for their anxiety-like phenotypes (Lewis and Tokyo WKY rats), or by exposure to stress or opiate withdrawal (Fox et al., 2015; McElligott et al., 2013). Those alterations were consistent with increased capacity for NA release into BNST. More recently, similar results were reported with combined FSCV and optogenetic stimulation in mice, where repeated restraint stress also significantly decreased the sensitivity of BNST NA release to the α_2-AR antagonist idazoxan (Schmidt et al., 2018). In another recent study, Deal and coworkers measured catecholamine efflux in BLA in response to electrical stimulation of LC (Deal et al., 2021). They did not find a reduced response to idazoxan, however, their recordings were made 5–7 days after the initial stressor (repeated social defeat or forced swim stress), which, as we show here, likely falls outside the transient window of α_2-AR adaptation. They did, however, report two more important findings. Firstly, that catecholamine release in BLA in stressed, but not naïve, rats, was responsive to D_2 antagonist raclopride, which the authors interpret in terms of an additional DA component. Secondly, that intraperitoneal administration of ethanol effectively reduced catecholamine efflux in BLA only in stressed, but not naïve subjects. Taken together, these data suggest that there are multiple adaptive changes in the joint DA–NA systems, possibly consisting of loss of α_2-AR (and, perhaps, also D_2R) sensitivity, increased catecholaminergic neuron activity, and transmitter release accompanied by decreased uptake. These alterations could have different temporal windows – especially given other studies showing that increased NA release and hyperactivity persist for at least 7 days after stress, therefore lasting longer than the putative α_2-AR adaptation (Borodovitsyna, Flamini, et al., 2018; Borodovitsyna, Joshi, et al., 2018; Ronzoni et al., 2016). In the context of the VTA, the implication is that for a limited time following a stressful experience, NA release into the VTA is likely potentiated, and thus the capacity of NA to modulate DA-ergic signaling is increased.

4.4 | Potential mechanisms of impaired α_2-AR regulation of NA efflux

While a loss in sensitivity at the α_2-AR after stress exposure has been experimentally well demonstrated in both rats and mice (Fox et al., 2015; McElligott et al., 2013; Schmidt et al., 2019), the molecular mechanism underlying this change has not yet been proposed. Here, we began to address this by testing whether stress affects receptor expression. We performed western blotting for both α_2-AR and D_2 receptors with the use of BS^3 crosslinking to attempt to separate the membrane-bound and intracellular fractions. However, no differences in total expression or membrane trafficking of either of those proteins were found between naïve and stressed animals based on this assay.

The two dominant subtypes of α_2-AR responsible for regulating NA release in the brain are α_{2A} and α_{2C} receptors, with α_{2A} being characterized as the subtype predominantly involved in transmitter regulation in conditions of high activity (Gilsbach & Hein, 2012; Hein et al., 1999). Our finding that both the total and membrane-bound fractions of the α_{2A} and D_2 receptors remain unchanged after stress is in agreement with findings in amphetamine-treated mice, where sensitization to high levels of catecholamines was accompanied by unchanged α_{2A} receptor binding in LC (Doucet et al., 2013). These data suggest that classical desensitization (receptor protein tagging by phosphorylation, followed by internalization) is not the predominant molecular pathway involved. Rather, it seems likely that changes in intracellular signaling, such as uncoupling from effector G proteins such as Ga1 and Ga2 (Doucet et al., 2013), or changes in interaction with other intracellular effectors, such as β-arrestin, could be implicated (Gilsbach & Hein, 2012). There is also the possibility that α_{2A} interacts with other receptors, such as NMDA glutamate receptors, as this interaction has been shown to attenuate NMDA-dependent excitatory transmission in retinal ganglion cells (Dong et al., 2008). Uncoupling of α_2-AR from such receptor–receptor interaction could be of relevance, as NMDA signaling is involved in driving LC activity, and at least some adaptations underlying drug sensitization are disrupted in the receptor subunit NR1 knockout mice – although here the picture is less clear due to potential compensatory changes in glutamate afferents in LC (Parkitna et al., 2012). It is also likely that D_2 receptors undergo similar adaptive changes, i.e. uncoupling from their G protein effector pathways, as this has also been demonstrated (Nimitvilai et al., 2013, 2014; Robinson et al., 2017). Ultimately, however, these are speculations based on prior studies in different systems and further research will be required to understand the source of adaptations in autoreceptor control over NA release in the brain.

4.5 | Caveats and outlook

Our results strongly suggest that NA-ergic modulation of the VTA is altered in response to stress, pointing to a potential novel locus for stress-related alterations in the catecholamine system. Stress-related

adaptations in the catecholaminergic systems could be relevant for affective and drug use disorders (Belujon & Grace, 2017; Caccamise et al., 2021; Koob, 2021; Sofuoglu & Sewell, 2009). With α_2-AR agonists being proposed for clinical use in the treatment of these disorders (Gowing et al., 2016; Sofuoglu et al., 2014; Upadhyay et al., 2021), a better understanding of neuroadaptations in the NA system across the brain could translate into future advances in treatment.

There are, however, several caveats and technical limitations which will need to be resolved before a firm conclusion is established. Firstly, the present study included only male rats. Similarly, prior studies showing reduced sensitivity at α_2-ARs either used male subjects (Fox et al., 2015, 2017; McElligott et al., 2013), or used counterbalancedd males and females, but did not report on sex differences in α_2-AR signaling and NA uptake (Schmidt et al., 2019). While demanding, obtaining detailed information about male/female variations in NA regulation after stress would be advantageous, as both NA and corticotropin systems exhibit sex differences in animals (Cason et al., 2016; den Hartog et al., 2020), and there is strong evidence for sex and gender as important factors influencing mental health outcomes in the clinic (Koob, 2021; Upadhyay et al., 2021). Secondly, while FSCV measurements performed in anesthetized rats in combination with pharmacological tools have provided valuable insights into catecholamine signaling in VTA, NAc, BNST, and BLA (Deal et al., 2021; Kielbinski et al., 2019; Park et al., 2017; Schmidt et al., 2019), insights from other techniques should be used to confirm and extend these findings. With the advent of novel fluorescent sensors for both NA and DA (Patriarchi et al., 2018; Sun et al., 2020), which are compatible with in-vivo fiber photometry, differentiating between catecholamines released at a single site, which is a longstanding challenge for FSCV, could be made possible. This technique is also more suited for recording in freely moving, awake animals, allowing for both verification of findings obtained in an anesthetized preparation, as well as studying the impact of α_2-AR alterations on behavior. Similarly, targeting select neuronal population for optogenetic manipulation could increase the specificity: while the role of the VTA-amygdala circuit in fear processing is well established (Jo et al., 2018; Luo et al., 2018; Tang et al., 2020), projections from neighboring areas, including A8 and A10 (Yetnikoff et al., 2014), could play a similar role, or, indeed, be recruited by electrical stimulation of the VTA. Finally, longer-term goals would include bringing these techniques together with the aim of clarifying the stressrelated mechanisms responsible for ostensible α_2-AR desensitization and establishing the relations between changes in NA transmission found in the VTA, BLA, BNST, and possibly other loci.

AUTHOR CONTRIBUTIONS

MK and JB planned and performed FSCV experiments, analyzed and presented the data and wrote the manuscript, JB and KZ performed behavioral procedures, JB and W-BA performed western blotting experiments, MM supervised western blotting experiments, reviewed and edited the manuscript, RP conceptualized, reviewed, and edited the manuscript; WS acquired funding, conceptualized, managed and supervised the projects as well as reviewed and edited the manuscript.

CONFLICT OF INTEREST

The authors have no conflict of interest to declare.

DATA AVAILABILITY STATEMENT

Data available on request from the authors.

ORCID

Wojciech Solecki https://orcid.org/0000-0002-0473-5472

REFERENCES

Arencibia-Albite, F., Paladini, C., Williams, J. T., & Jiménez-Rivera, C. A. (2007). Noradrenergic modulation of the hyperpolarization-activated cation current (Ih) in dopamine neurons of the ventral tegmental area. *Neuroscience*, *149*, 303–314.

Aston-Jones, G., & Harris, G. C. (2004). Brain substrates for increased drug seeking during protracted withdrawal. *Neuropharmacology*, *47*, 167–179.

Baik, J.-H. (2020). Stress and the dopaminergic reward system. *Experimental & Molecular Medicine*, *52*, 1879–1890.

Bator, E., Latusz, J., Głowacka, U., Radaszkiewicz, A., Mudlaff, K., & Maćkowiak, M. (2018). Adolescent social isolation affects schizophrenia-like behavior in the MAM-E17 model of schizophrenia. *Neurotoxicity Research*, *34*, 305–323.

Beier, K. T., Steinberg, E. E., DeLoach, K. E., Xie, S., Miyamichi, K., Schwarz, L., Gao, X. J., Kremer, E. J., Malenka, R. C., & Luo, L. (2015). Circuit architecture of VTA dopamine neurons revealed by systematic input-output mapping. *Cell*, *162*, 622–634.

Belujon, P., & Grace, A. A. (2017). Dopamine system dysregulation in major depressive disorders. *The International Journal of Neuropsychopharmacology*, *20*, 1036–1046.

Borodovitsyna, O., Flamini, M. D., & Chandler, D. J. (2018). Acute stress persistently alters locus coeruleus function and anxiety-like behavior in adolescent rats. *Neuroscience*, *373*, 7–19.

Borodovitsyna, O., Joshi, N., & Chandler, D. (2018). Persistent stress-induced neuroplastic changes in the locus coeruleus/norepinephrine system. *Neural Plasticity*, *2018*, 1–14.

Boudreau, A. C., Milovanovic, M., Conrad, K. L., Nelson, C., Ferrario, C. R., & Wolf, M. E. (2012). A protein cross-linking assay for UNIT 5.30 measuring cell surface expression of glutamate receptor subunits in the rodent brain after in vivo treatments.

Boudreau, A. C., & Wolf, M. E. (2005). Behavioral sensitization to cocaine is associated with increased AMPA receptor surface expression in the nucleus Accumbens. *The Journal of Neuroscience*, *25*, 9144–9151.

Bucher, E. S., Brooks, K., Verber, M. D., Keithley, R. B., Owesson-White, C., Carroll, S., Takmakov, P., McKinney, C. J., & Wightman, R. M. (2013). Flexible software platform for fast-scan cyclic voltammetry data acquisition and analysis. *Analytical Chemistry*, *85*, 10344–10353.

Caccamise, A., Newenhizen, E. V., & Mantsch, J. R. (2021). *Neurochemical mechanisms and neurocircuitry underlying the contribution of stress to cocaine seeking.* John Wiley and Sons Inc.

Cason, A. M., Kohtz, A., & Aston-Jones, G. (2016). Role of corticotropin releasing factor 1 signaling in cocaine seeking during early extinction in female and male rats. *PLoS One*, 11, 1–12.

Chocyk, A., Bobula, B., Dudys, D., Przyborowska, A., Majcher-Maślanka, I., Hess, G., & Wedzony, K. (2013). Early-life stress affects the structural and functional plasticity of the medial prefrontal cortex in adolescent rats. *The European Journal of Neuroscience*, 38, 2089–2107.

Daviu, N., Bruchas, M. R., Moghaddam, B., Sandi, C., & Beyeler, A. (2019). Neurobiological links between stress and anxiety. *Neurobiology of Stress*, 11, 100191.

de la Mora, M. P., Gallegos-Cari, A., Arizmendi-García, Y., Marcellino, D., & Fuxe, K. (2010). Role of dopamine receptor mechanisms in the amygdaloid modulation of fear and anxiety: Structural and functional analysis. *Progress in Neurobiology*, 90, 198–216.

Deal, A. L., Park, J., Weiner, J. L., & Budygin, E. A. (2021). Stress alters the effect of alcohol on catecholamine dynamics in the basolateral amygdala. *Frontiers in Behavioral Neuroscience*, 15, 1–10.

den Hartog, C. R., Blandino, K. L., Nash, M. K. L., Sjogren, E. R., Grampetro, M. A., Moorman, D. E., & Vazey, E. M. (2020). Noradrenergic tone mediates marble burying behavior after chronic stress and ethanol. *Psychopharmacology*, 237, 3021–3031.

Dong, C. J., Guo, Y., Agey, P., Wheeler, L., & Hare, W. A. (2008). α2 adrenergic modulation of NMDA receptor function as a major mechanism of RGC protection in experimental glaucoma and retinal excitotoxicity. *Investigative Ophthalmology and Visual Science*, 49, 4515–4522.

Doucet, E. L., Bobadilla, A. C., Houades, V., Lanteri, C., Godeheu, G., Lanfumey, L., Sara, S. J., & Tassin, J. P. (2013). Sustained impairment of α2A-adrenergic autoreceptor signaling mediates neurochemical and behavioral sensitization to amphetamine. *Biological Psychiatry*, 74, 90–98.

Douma, E. H., & de Kloet, E. R. (2020). Stress-induced plasticity and functioning of ventral tegmental dopamine neurons. *Neuroscience and Biobehavioral Reviews*, 108, 48–77.

Field, K. J., White, W. J., & Lang, C. M. (1993). Anaesthetic effects of chloral hydrate, pentobarbitone and urethane in adult male rats. *Laboratory Animals*, 27, 258–269.

Fox, M. E., Rodeberg, N. T., & Wightman, R. M. (2017). Reciprocal catecholamine changes during opiate exposure and withdrawal. *Neuropsychopharmacology*, 42, 671–681.

Fox, M. E., Studebaker, R. I., Swofford, N. J., & Wightman, R. M. (2015). Stress and drug dependence differentially modulate norepinephrine signaling in animals with varied HPA axis function. *Neuropsychopharmacology*, 40, 1752–1761.

Garris, P. A., Wightman, R. M., Hill, C., & Carolina, N. (1994). Different kinetics govern dopaminergic transmission in the amygdala, prefrontal cortex, and striatum: An in vivo voltammetric study. *The Journal of Neuroscience*, 14, 442–450.

Gilsbach, R., & Hein, L. (2012). Are the pharmacology and physiology of α 2adrenoceptors determined by α 2-heteroreceptors and autoreceptors respectively? *British Journal of Pharmacology*, 165, 90–102.

Giustino, T. F., & Maren, S. (2018). Noradrenergic modulation of fear conditioning and extinction. *Frontiers in Behavioral Neuroscience*, 12, 1–20.

Goertz, R. B., Wanat, M. J., Gomez, J. A., Brown, Z. J., Phillips, P. E., & Paladini, C. A. (2015). Cocaine increases dopaminergic neuron and motor activity via midbrain α1 adrenergic signaling. *Neuropsychopharmacology*, 40, 1151–1162.

Gowing, L., Farrell, M., Ali, R., & White, J. M. (2016). *Alpha2-adrenergic agonists for the management of opioid withdrawal.* The Cochrane Database of Systematic Reviews.

Grenhoff, J., North, R. A., & Johnson, S. W. (1995). Alpha$_1$ -adrenergic effects on dopamine neurons recorded intracellularly in the rat midbrain slice. *The European Journal of Neuroscience*, 7, 1707–1713.

Guiard, B. P., Mansari, M. E., & Blier, P. (2008). Cross-talk between dopaminergic and noradrenergic systems in the rat ventral tegmental area, locus ceruleus, and dorsal hippocampus. *Molecular Pharmacology*, 74, 1463–1475.

Haubrich, J., Bernabo, M., & Nader, K. (2020). Noradrenergic projections from the locus coeruleus to the amygdala constrain fear memory reconsolidation. *eLife*, 9, 1–29.

Hein, L., Altman, J. D., & Kobilka, B. K. (1999). Two functionally distinct α2-adrenergic receptors regulate sympathetic neurotransmission. *Nature*, 402, 181–184.

Holloway, Z. R., Freels, T. G., Comstock, J. F., Nolen, H. G., Sable, H. J., & Lester, D. B. (2019). Comparing phasic dopamine dynamics in the striatum, nucleus accumbens, amygdala, and medial prefrontal cortex. *Synapse*, 73, 1–15.

Janak, P. H., & Tye, K. M. (2015). From circuits to behaviour in the amygdala. *Nature*, 517, 284–292.

Jo, Y. S., Heymann, G., & Zweifel, L. S. (2018). Dopamine neurons reflect the uncertainty in fear generalization. *Neuron*, 100, 916–925.e3.

Keithley, R. B., & Wightman, R. M. (2011). Assessing principal component regression prediction of neurochemicals detected with fast-scan cyclic voltammetry. *ACS Chemical Neuroscience*, 2, 514–525.

Kielbinski, M., Bernacka, J., & Solecki, W. B. (2019). Differential regulation of phasic dopamine release in the forebrain by the VTA noradrenergic receptor signaling. *Journal of Neurochemistry*, 149, 747–759.

Koob, G. F. (2014). Neurocircuitry of alcohol addiction. In *Handbook of clinical neurology* (Vol. 125, pp. 33–54). Elsevier B.V.

Koob, G. F. (2021). Drug addiction: Hyperkatifeia/negative reinforcement as a framework for medications development. *Pharmacological Reviews*, 73, 163–201.

Koob, G. F., Buck, C. L., Cohen, A., Edwards, S., Park, P. E., Schlosburg, J. E., Schmeichel, B., Vendruscolo, L. F., Wade, C. L., Whitfield, T. W., Jr., & George, O. (2014). Addiction as a stress surfeit disorder. *Neuropharmacology*, 76, 370–382.

Kwon, O. B., Lee, J. H., Kim, H. J., Lee, S., Lee, S., Jeong, M. J., Kim, S. J., et al. (2015). Dopamine regulation of amygdala inhibitory circuits for expression of learned fear. *Neuron*, 88, 378–389.

Lee, J. H., Lee, S., & Kim, J. H. (2017). *Amygdala circuits for fear memory: A key role for dopamine regulation.* SAGE Publications Inc.

Luo, R., Uematsu, A., Weitemier, A., Aquili, L., Koivumaa, J., McHugh, T. J., & Johansen, J. P. (2018). A dopaminergic switch for fear to safety transitions. *Nature Communications*, 9, 1–11.

McCall, J. G., Al-Hasani, R., Siuda, E. R., Hong, D. Y., Norris, A. J., Ford, C. P., & Bruchas, M. R. (2015). CRH engagement of the locus coeruleus noradrenergic system mediates stress-induced anxiety. *Neuron*, 87, 605–620.

McCall, J. G., Siuda, E. R., Bhatti, D. L., Lawson, L. A., McElligott, Z. A., Stuber, G. D., & Bruchas, M. R. (2017). Locus coeruleus to basolateral amygdala noradrenergic projections promote anxiety-like behavior. *eLife*, 6, 1–23.

McElligott, Z. A., Fox, M. E., Walsh, P. L., Urban, D. J., Ferrel, M. S., Roth, B. L., & Wightman, R. M. (2013). Noradrenergic synaptic function in the bed nucleus of the stria terminalis varies in animal models of anxiety and addiction. *Neuropsychopharmacology*, 38, 1665–1673.

Mejias-Aponte, C. A. (2016). Specificity and impact of adrenergic projections to the midbrain dopamine system. *Brain Research*, 1641, 258–273.

Mejías-Aponte, C. A., Drouin, C., & Aston-Jones, G. (2009). Adrenergic and noradrenergic innervation of the midbrain ventral tegmental area and retrorubral field: Prominent inputs from medullary homeostatic centers. *The Journal of Neuroscience*, 29, 3613–3626.

Morilak, D. A., Barrera, G., Echevarria, D. J., Garcia, A. S., Hernandez, A., Ma, S., & Petre, C. O. (2005). Role of brain norepinephrine in the behavioral response to stress. *Progress in Neuro-Psychopharmacology & Biological Psychiatry*, 29, 1214–1224.

Nimitvilai, S., Herman, M., You, C., Arora, D. S., McElvain, M. A., Roberto, M., & Brodie, M. S. (2014). Dopamine D2 receptor desensitization

by dopamine or corticotropin releasing factor in ventral tegmental area neurons is associated with increased glutamate release. *Neuropharmacology*, 82, 28–40.

Nimitvilai, S., McElvain, M. A., & Brodie, M. S. (2013). Reversal of dopamine D2 agonist-induced inhibition of ventral tegmental area neurons by Gq-linked neurotransmitters is dependent on protein kinase C, G protein-coupled receptor kinase, and dynamin. *The Journal of Pharmacology and Experimental Therapeutics*, 344, 253–263.

Paladini, C. A., Fiorillo, C. D., Morikawa, H., & Williams, J. T. (2001). Amphetamine selectively blocks inhibitory glutamate transmission in dopamine neurons. *Nature Neuroscience*, 4, 275–281.

Park, J. W., Bhimani, R. V., & Park, J. (2017). Noradrenergic modulation of dopamine transmission evoked by electrical stimulation of the locus coeruleus in the rat brain. *ACS Chemical Neuroscience*, 8, 1913–1924.

Parkitna, J. R., Solecki, W., Gołembiowska, K., Tokarski, K., Kubik, J., Gołda, S., Novak, M., Parlato, R., Hess, G., Sprengel, R., & Przewłocki, R. (2012). Glutamate input to noradrenergic neurons plays an essential role in the development of morphine dependence and psychomotor sensitization. *The International Journal of Neuropsychopharmacology*, 15, 1457–1471.

Patriarchi, T., Cho, J. R., Merten, K., Howe, M. W., Marley, A., Xiong, W. H., Folk, R. W., Broussard, G. J., Liang, R., Jang, M. J., Zhong, H., Dombeck, D., von Zastrow, M., Nimmerjahn, A., Gradinaru, V., Williams, J. T., & Tian, L. (2018). Ultrafast neuronal imaging of dopamine dynamics with designed genetically encoded sensors. *Science*, 360(6396), eaat4422.

Paxinos, G., & Watson, C. (2013). *The rat brain in stereotaxic coordinates*. Amsterdam Academic Press.

Poulin, J.-F., Caronia, G., Hofer, C., Cui, Q., Helm, B., Ramakrishnan, C., Chan, C. S., Dombeck, D. A., Deisseroth, K., & Awatramani, R. (2018). Mapping projections of molecularly defined dopamine neuron subtypes using intersectional genetic approaches. *Nature Neuroscience*, 21, 1260–1271.

Robinson, B. G., Bunzow, J. R., Grimm, J. B., Lavis, L. D., Dudman, J. T., Brown, J., Neve, K. A., & Williams, J. T. (2017). Desensitized D2 autoreceptors are resistant to trafficking. *Scientific Reports*, 7, 1–14.

Rodeberg, N. T., Johnson, J. A., Cameron, C. M., Saddoris, M. P., Carelli, R. M., & Wightman, R. M. (2015). Construction of training sets for valid calibration of in vivo cyclic Voltammetric data by principal component analysis. *Analytical Chemistry*, 87, 11484–11491.

Ronzoni, G., del Arco, A., Mora, F., & Segovia, G. (2016). Enhanced noradrenergic activity in the amygdala contributes to hyperarousal in an animal model of PTSD. *Psychoneuroendocrinology*, 70, 1–9.

Sánchez-Soto, M., Bonifazi, A., Cai, N. S., Ellenberger, M. P., Newman, A. H., Ferré, S., & Yano, H. (2016). Evidence for noncanonical neurotransmitter activation: Norepinephrine as a dopamine D2-like receptor agonist. *Molecular Pharmacology*, 89, 457–466.

Schmidt, K. T., Makhijani, V. H., Boyt, K. M., Cogan, E. S., Pati, D., Pina, M. M., Bravo, I. M., Locke, J. L., Jones, S. R., Besheer, J., & McElligott, Z. A. (2019). Stress-induced alterations of norepinephrine release in the bed nucleus of the stria terminalis of mice. *ACS Chemical Neuroscience*, 10, 1908–1914.

Schmidt, K. T., Makhijani, V. H., Boyt, K. M., Cogan, E. S., Pati, D., Pina, M. M., Bravo, I. M., et al. (2018). *Stress-induced alterations of norepinephrine release in the bed nucleus of the stria terminalis of mice*. ACS Chemical Neuroscience.

Schneider, C. A., Rasband, W. S., & Eliceiri, K. W. (2012). NIH image to ImageJ: 25 years of image analysis. *Nature Methods*, 9, 671–675.

Schwarz, L. A., & Luo, L. (2015). Organization of the locus coeruleus-norepinephrine system. *Current Biology*, 25, R1051–R1056.

Sharp, B. M. (2017). Basolateral amygdala and stress-induced hyperexcitability affect motivated behaviors and addiction. *Translational Psychiatry*, 7, e1194.

Shnitko, T. A., & Robinson, D. L. (2014). Anatomical and pharmacological characterization of catecholamine transients in the medial prefrontal cortex evoked by ventral tegmental area stimulation. *Synapse*, 68, 131–143.

Smith, R. J., & Aston-Jones, G. (2008). Noradrenergic transmission in the extended amygdala: Role in increased drug-seeking and relapse during protracted drug abstinence. *Brain Structure & Function*, 213, 43–61.

Sofuoglu, M., Rosenheck, R., & Petrakis, I. (2014). Pharmacological treatment of comorbid PTSD and substance use disorder: Recent progress. *Addictive Behaviors*, 39, 428–433.

Sofuoglu, M., & Sewell, R. A. (2009). Norepinephrine and stimulant addiction. *Addiction Biology*, 14, 119–129.

Solecki, W. B., Kielbinski, M., Karwowska, K., Zajda, K., Wilczkowski, M., Rajfur, Z., & Przewłocki, R. (2019). Alpha 1–adrenergic receptor blockade in the ventral tegmental area modulates conditional stimulus-induced cocaine seeking. *Neuropharmacology*, 158, 107680.

Solecki, W. B., Szklarczyk, K., Klasa, A., Pradel, K., Dobrzański, G., & Przewłocki, R. (2017). Alpha 1-adrenergic receptor blockade in the VTA modulates fear memories and stress responses. *European Neuropsychopharmacology*, 27, 782–794.

Solecki, W. B., Szklarczyk, K., Pradel, K., Kwiatkowska, K., Dobrzański, G., & Przewłocki, R. (2018). Noradrenergic signaling in the VTA modulates cocaine craving. *Addiction Biology*, 23, 596–609.

Stubbendorff, C., & Stevenson, C. W. (2021). Dopamine regulation of contextual fear and associated neural circuit function. *The European Journal of Neuroscience*, 54, 6933–6947.

Sun, F., Zhou, J., Dai, B., Qian, T., Zeng, J., Li, X., Zhuo, Y., Zhang, Y., Wang, Y., Qian, C., Tan, K., Feng, J., Dong, H., Lin, D., Cui, G., & Li, Y. (2020). Next-generation GRAB sensors for monitoring dopaminergic activity in vivo. *Nature Methods*, 17, 1156–1166.

Tang, W., Kochubey, O., Kintscher, M., & Schneggenburger, R. (2020). A VTA to basal amygdala dopamine projection contributes to signal salient somatosensory events during fear learning. *The Journal of Neuroscience*, 40, 3969–3980.

Tovar-Díaz, J., Pomrenze, M. B., Kan, R., Pahlavan, B., & Morikawa, H. (2018). Cooperative CRF and α1 adrenergic signaling in the VTA promotes NMDA plasticity and drives social stress enhancement of cocaine conditioning. *Cell Reports*, 22, 2601–2614.

Upadhyay, J., Verrico, C. D., Cay, M., Kodele, S., Yammine, L., Koob, G. F., & Schreiber, R. (2021). Neurocircuitry basis of the opioid use disorder–post-traumatic stress disorder comorbid state: Conceptual analyses using a dimensional framework. *The Lancet Psychiatry*, 0366, 1–13.

Velásquez-Martinez, M. C., Santos-Vera, B., Velez-Hernandez, M. E., Vazquez-Torres, R., & Jimenez-Rivera, C. A. (2020). Alpha-1 adrenergic receptors modulate glutamate and GABA neurotransmission onto ventral tegmental dopamine neurons during cocaine sensitization. *International Journal of Molecular Sciences*, 21, 790.

Velásquez-Martinez, M. C., Vázquez-Torres, R., & Jiménez-Rivera, C. A. (2012). Activation of alpha1-adrenoceptors enhances glutamate release onto ventral tegmental area dopamine cells. *Neuroscience*, 216, 18–30.

Velásquez-Martínez, M. C., Vázquez-Torres, R., Rojas, L. V., Sanabria, P., & Jiménez-Rivera, C. A. (2015). Alpha-1 adrenoreceptors modulate GABA release onto ventral tegmental area dopamine neurons. *Neuropharmacology*, 88, 110–121.

Wickham, R., Solecki, W., Rathbun, L., McIntosh, J. M., & Addy, N. A. (2013). Ventral tegmental area α6β2 nicotinic acetylcholine receptors modulate phasic dopamine release in the nucleus accumbens core. *Psychopharmacology*, 229, 73–82.

Williams, M. A., Li, C., Kash, T. L., Matthews, R. T., & Winder, D. G. (2014). Excitatory drive onto dopaminergic neurons in the rostral linear nucleus is enhanced by norepinephrine in an α1 adrenergic receptor-dependent manner. *Neuropharmacology*, 86, 116–124.

Yetnikoff, L., Lavezzi, H. N., Reichard, R. A., & Zahm, D. S. (2014). An update on the connections of the ventral mesencephalic dopaminergic complex. *Neuroscience*, *282*, 23–48.

SUPPORTING INFORMATION

Additional supporting information can be found online in the Supporting Information section at the end of this article.